CONF-810429--5

LA-UR-81-994

TITLE: A WHISPERING-MODE WAVEGUIDE

MASTER

AUTHOR(S): N. A. Kurnit

SUBMITTED TO: Los Alamos Optics Conference 1981
Santa Fe, NM - April 7-10, 1981

University of California

LOS ALAMOS SCIENTIFIC LABORATORY
Post Office Box 1663 Los Alamos, New Mexico 87545
An Affirmative Action/Equal Opportunity Employer

Form No. 836 R3
St. No. 2629
12/78

UNITED STATES
DEPARTMENT OF ENERGY
CONTRACT W-7405-ENG. 36

A WHISPERING-MODE WAVEGUIDE

N. A. Kurnit
University of California
Los Alamos National Laboratory
P. O. Box 1663
Los Alamos, New Mexico 87545

ABSTRACT

Properties of a relatively new type of waveguide structure of potential use for confining infrared radiation to a small mode volume over long path lengths are reviewed. A single guiding surface with curvature radius ρ and band radius R allows propagation of a near-grazing incidence "whispering mode" of transverse width $\sim(\lambda \sqrt{\rho R}/\pi)^{1/2}$ and radial width $\sim 1/2\ (\lambda^2 R)^{1/3}$. For sufficiently large ρ, the loss per revolution for TE mode propagation is $\sim\pi A_N$, where A_N is the normal-incidence reflection loss. Results on a number of prototype structures in general agreement with these considerations is described.

INTRODUCTION

It is often desirable, particularly for infrared and longer wavelengths, to confine radiation to a small mode volume over distances long compared to the distance for which diffraction spreading is appreciable. Hollow dielectric waveguides[1] have been used for such confinement and have had numerous applications to the development of discharge-pumped lasers.[2] They have also been used for absorption spectroscopy,[3] optical pumping,[4] and stimulated Raman scattering.[5,6] Very long lengths of such waveguides are cumbersome and difficult to construct; however, particularly since tight tolerances on straightness are required in order to prevent mode conversion into lossy higher-order modes.

Bent rectangular metallic waveguides have been extensively studied[7-11] as a means of steering CO_2 laser radiation for cutting, welding, and surgery. Their principal disadvantage is that the walls perpendicular to the electric field give a relatively large attenuation coefficient. In the case of straight metallic waveguides, it has been demonstrated, however, that these walls may be removed completely if the walls parallel to the electric field are given a slight curvature which keeps the mode focused in the center of the guide.[12-14] If one combines this concept with that of a waveguide bent in a circle, spiral, or helix, one has a structure which can be made in long lengths yet fit into a compact volume. Moreover, due to the propensity of light to travel in straight lines, the wave remains confined in the region near the outer wall even if the inner wall is removed. This greatly simplifies the fabrication problem since only a single curved boundary is required, as illustrated in Fig. 1. The radial intensity distribution of the modes of such a system in the limiting case of a cylinder were originally discussed by Lord Rayleigh[15-17] in connection

with the "whispering gallery" phenomenon in St. Paul's Cathedral, and will be described in sec. II. The toroidal geometry described above has previously been proposed[18-21] for flexible guiding of CO_2 laser radiation and has been applied to the construction of a CO_2 laser.[20] The transverse mode profile derived in sec. III by a simple lens waveguide approach is in substantial agreement with the results obtained by these authors from an approximate solution of the wave equation.

Results obtained on some prototype structures are described in the experimental section. These results agree quite closely with theoretical predictions and indicate that it should be possible to build quite long "whispering-mode" waveguides with sufficiently low loss to be of interest for optically pumped and Raman lasers and for spectroscopic applications. A circular structure, closed except for a hole or other perturbation provided for input or output coupling, could be used as a true "ring"[22-25] resonator.

Other possible applications include use as an optical delay line. Short sections might be applicable to the study of adsorbed molecules[26] or thin surface films[27,28] if used with E polarized perpendicular to the surface. A cylindrical surface of a relatively absorbing material turned inward in a single spiral turn could provide a convenient beam dump or calorimeter for high power laser radiation since the radiation would be absorbed over a large surface area after many reflections, and very little scattered light would be able to exit from the device.

II. RADIAL MODE PROPERTIES

It is convenient to first consider the modes of a cylindrical system, with no confinement of the mode in the transverse direction. It is shown

in Ref. 9 that for a sufficiently small bend radius, R, the mode amplitude at the inner wall of a bent waveguide becomes vanishingly small, and the mode propagates by reflections off only the outer wall. Under these conditions (to be quantified shortly), the inner wall can be removed, and in a geometrical optics description, a ray can be pictured as making successive reflections at angle θ with the respect to the tangent to the surface, as shown in Fig. 2. Garmire[29] has demonstrated that the waveguide attenuation coefficient[1,13,30] can be derived from consideration of the angle which a ray makes with the wall and the angular dependence of the Fresnel reflection coefficient, and this insight has been used to deduce the remarkable result[9] that the loss of a TE wave (E perpendicular to the plane of incidence) in a bent metallic guide depends only on the angle through which the beam is turned and the reflectivity, independent of the bend radius. This follows from the fact that for a highly reflecting metal with refractive index $\nu = \eta - i\kappa$, the amplitude reflection coefficient for the TE wave is given by[31]

$$r_s = \frac{\sqrt{\nu^2 - \cos^2\theta} - \sin\theta}{\sqrt{\nu^2 - \cos^2\theta} + \sin\theta} \simeq \frac{\nu - \sin\theta}{\nu + \sin\theta} \quad , \tag{1}$$

where the approximation on the right results from $|\mathrm{Re}(\nu^2)| = |\eta^2 - \kappa^2| \gg 1$. For well-prepared surfaces of copper at 10.6 μm, $\eta = 12$, $\kappa = 63$[32] and $|\eta^2 - \kappa^2| \simeq 4000$, so the validity of the approximation is excellent, and it becomes exact for normal incidence ($\theta = 90°$). The reflection loss is thus

$$A^{TE}(\theta) = 1 - |r_s|^2 \cong \frac{4\,\mathrm{Re}\,(\nu)\,\sin\theta}{|\nu + \sin\theta|^2} \qquad (2)$$

If sin θ in the denominator is neglected in comparison with ν, so that the normal incidence absorptance $A_N = 4\,\mathrm{Re}(\nu)/|\nu + 1|^2$ is approximated by $A_N \cong 4\,\mathrm{Re}\,(1/\nu)$, Eq. 2 becomes

$$A^{TE}(\theta) \cong 4\,\mathrm{Re}\,(1/\nu)\,\sin\theta \cong A_N \sin\theta \qquad (2a)$$

Similarly, one has for the TM wave

$$A^{TM}(\theta) \cong \frac{4\,\mathrm{Re}\,(\nu)\,\sin\theta}{|\,\nu\sin\theta + 1|^2} \quad . \qquad (3)$$

The term ν sin θ in the denominator can be neglected only for very small angles; in copper at 10 μm the TM loss increases very rapidly to ~50% at $\theta \simeq 0.8°$, and then decreases more gradually for larger angle. For a very small range of angles near grazing incidence, Eq. (3) can be approximated by

$$A^{TM}(\theta) \simeq 4\,\mathrm{Re}(\nu)\,\sin\theta = (\eta^2 + \kappa^2)\,A^{TE}(\theta) \quad . \qquad (3a)$$

The light polarized in the plane of incidence is thus ~4000 times more lossy than the light polarized perpendicular to the plane of incidence in the limit of very small angles; angles small enough for Eq. 3a to be valid will not generally be the case, however.

From Fig. 2, we see that the number of bounces to turn the beam through an angle φ is φ/2θ, so the TE loss in bending the beam through angle φ is, in the limit of small losses,[11,33,34]

$$A_B(\phi) = (\phi/2\theta)\, A^{TE}(\theta) = (\phi/2\theta)\, A_N \sin\theta \simeq A_N\phi/2 \quad , \qquad (4)$$

which, as stated earlier, is independent of R and θ, within the approximations made. Thus for a complete revolution, the loss is predicted to be $\sim\pi\, A_N$, which can be quite small. It is interesting to note that the loss per unit length for a circle of diameter d is nearly the same as that for two mirrors of the same material separated by distance d. However, the energy absorbed per unit area is much lower in the waveguide since the beam is spread out on the surface by a factor of 1/sin θ and the absorption is reduced by an additional factor of sin θ, so that the waveguide walls can confine a mode with energy density $\sim 1/\sin^2\theta$ times greater than would damage a normal-incidence mirror.

The existence of well-defined whispering modes of propagation in a cylindrical cavity was first discussed by Lord Rayleigh,[16] who pointed out that any field distribution could be expanded in terms of the wave functions

$$\psi_n = J_n(kr)\, e^{-i(\omega t - n\phi)} \quad , \; n = 0, \pm 1, \pm 2 \ldots \qquad (5)$$

where $J_n(kr)$ is a Bessel function of order n, and $k = 2\pi/\lambda$. For the modes of interest, the order number n, which is also the number of wavelengths which fit inside the circumference, is very large, and J_n remains very small until kr approaches n. It is shown in Ref. (16) that for the boundary condition $J_n(kR) = 0$ corresponding to the TE wave on a perfectly conducting surface, the solution for the first zero is

$$kR = \frac{2\pi R}{\lambda} \cong n + 1.86\, n^{1/3} \quad , \qquad (6)$$

while the function reaches a maximum for

$$kr \cong n + 0.51\, n^{1/3} \tag{7}$$

and falls to a negligible value for

$$kr \cong n - 1.5\, n^{1/3} \quad . \tag{8}$$

Thus nearly all of the energy is confined within a range Δr from the wall such that $k\Delta r \sim 3.4\, n^{1/3} \sim 3.4\, (kR)^{1/3}$, or

$$\Delta r \cong (\lambda^2 R)^{1/3} \quad . \tag{9}$$

The physical significance of Eq. (6) is that the average distance traveled by the wave is smaller than $2\pi R$ by an amount which scales as $(\lambda^2 R)^{1/3} \sim \lambda n^{1/3}$. The TM wave has a maximum of J_n at the wall and is thus confined to an even thinner region near the wall; the corresponding solution is[16]

$$kR = n + 0.81\, n^{1/3} \quad . \tag{10}$$

Higher-order modes correspond to higher zeros of J_n or J_n' at the wall and approximate analytic solutions have been derived for these eigenvalues:[35]

$$\text{TE:} \quad kR = n + \frac{n^{1/3}}{2} \left[3\pi\,(m - 1/4)\right]^{2/3} + \ldots, \quad m = 1,2 \ldots \tag{11a}$$

$$\text{TM:} \quad kR = n + \frac{n^{1/3}}{2} \left[3\pi\,(m - 3/4)\right]^{2/3} + \ldots, \quad m = 1,2 \ldots \tag{11b}$$

Because of the difficulty of computing these Bessel functions of large n, this problem has also been treated[24,34] by means of a conformal transformation[36] to a straight section bounding a medium with exponentially varying index of refraction. Approximate solutions for all the modes obtained by these and other techniques[18,21] are given by the Airy function;[37] this solution is also obtained for the related problem of atmospheric propagation of radio waves guided by an inversion layer.[38,39] The amplitudes of the TE mode of order m is given (aside from a normalization factor) by[38,33,20,21]

$$E_m = \mathrm{Ai}\left[\left(\frac{2k^2}{R}\right)^{1/3} (R - r) + \xi_m\right] \tag{12a}$$

where[40]

$$\xi_m \cong -\left[\frac{3\pi}{2}\left(m - \frac{1}{4}\right)\right]^{2/3} \tag{12b}$$

is the m^{th} zero of Ai(x). Each mode corresponds to the conducting wall being placed at different values of ξ_m, as indicated in Fig. 3. The distance between the wall and the inflection point at Ai(0) can be used as a measure of the width of the mode; setting the argument of Ai in Eq. (12a) equal to zero yields for this width[41,9]

$$a_b = \frac{1}{2}\lambda^2 R^{1/3}\left[\frac{3}{2}\left(m - \frac{1}{4}\right)\right]^{2/3} \tag{13}$$

The analysis in Ref. (38) also gives a value for the angle θ at which a ray is incident on the surface:

$$\sin^3\theta = \frac{3}{2}\frac{\lambda}{R}\left(m - \frac{1}{4}\right) \tag{14}$$

The TM wave has corresponding solutions with a maximum at the wall and the factor 1/4 in Eqs. 12-14 replaced by 3/4.

Some insight into the physical origin of the last two relations, at least for the lowest order (m = 1) mode, can be obtained by asking how a Gaussian TEM_o beam should be focused so that it remains in the thinnest possible annulus near the wall. From Fig. 2 we see that if a beam is focused at a distance δ from the wall, all rays within an angle of $\pm\,\alpha$ of the central ray will remain at a distance from the axis greater than $R_o = (R - \delta)\cos\alpha$.[15] If we take α to be the diffraction half-angle of a Gaussian beam focused to a waist with E-field 1/e radius w_o, $\alpha = \lambda/\pi w_o$, expand cos α for small α and write $\delta = pw_o$, the radius R_o is given by

$$R_o = R - pw_o - \frac{\lambda^2 R}{2\pi^2 w_o} + \text{smaller terms.} \tag{15}$$

Maximizing this expression with respect to w_o gives

$$w_o^3 = \frac{\lambda^2 R}{p\pi^2} \tag{16}$$

and

$$R - R_o = \frac{3}{2}\left(\frac{p}{\pi}\right)^{2/3}(\lambda^2 R)^{1/3} . \tag{17}$$

Thus we see that the $(\lambda^2 R)^{1/3}$ scaling of the mode size results from the competing effect of diffraction as the beam is focused more tightly in order to bring it closer to the wall. The quantity $p = \delta/w_o$ should be taken as small as possible without clipping significant energy from the beam; this requires $p \gtrsim 1.5$.

An expression for sin θ also follows by noting that $\delta = pw_o = (L/2)^2/2R$, where L is the chord length in Fig. 2, or

$$L/2 = \left(2pRw_o\right)^{1/2} \quad . \tag{18}$$

Thus

$$\sin\theta = \frac{L/2}{R} = \left(\frac{2pw_o}{R}\right)^{1/2} \tag{19}$$

and, using Eq. 16,

$$\sin\theta = \sqrt{2}\left(\frac{p}{\pi}\ \frac{\lambda}{R}\right)^{1/3} \quad . \tag{20}$$

This result agrees with Eq. 14 if we take $p = (9/8)(\pi/2^{3/2}) = 1.25$. It is not surprising that the Gaussian must be crowded close enough to the wall to have some energy clipped from it to give the same value of θ as the actual mode, since, as seen in Fig. 3, this mode rises much more steeply near the wall than a Gaussian. A Gaussian will always excite a superposition of modes; methods of coupling more nearly into a single mode are described in the experimental section.

III. Transverse Mode Properties

The discussion has thus far been limited to a cylindrical surface which provides no confinement of the mode in the transverse direction. The effect of adding a curvature with radius ρ to the cylindrical surface as shown in Fig. 4 is most readily analyzed by means of a standard lens waveguide approach[42,43] commonly used for analysis of laser cavity modes. Referring to Fig. 4, the focal length experienced by a transverse (sagittal) bundle of rays incident at angle θ on the surface is[44]

$$f = \frac{\rho/2}{\sin \theta} \tag{21}$$

and the distance at which the rays next meet the surface is

$$L = 2R \sin \theta \quad . \tag{22}$$

The g parameter for the equivalent lens waveguide is defined as

$$g \equiv 1 - \frac{L}{2f} = 1 - 2 \frac{R}{\rho} \sin \theta \quad , \tag{23}$$

and stable modes exist provided $-1 < g < 1$. The modes of greatest interest here have a small variation in size between bounces, which requires $g \simeq 1$, or

$$\sin^2 \theta << \frac{\rho}{2R} \tag{24}$$

This is easily satisfied, and for values of θ given by Eq. (14), this condition is met provided $\rho >> 2 (\lambda^2 R)^{1/3}$.

The lowest order transverse mode solution for this equivalent lens waveguide is a Gaussian beam with waist size[45]

$$w_o = \left(\frac{L\lambda}{2\pi}\right)^{1/2} \left(\frac{1+g}{1-g}\right)^{1/4}$$

$$= \left(\frac{\lambda\sqrt{\rho R}}{\pi}\right)^{1/2} \left(1 - \frac{R}{\rho}\sin^2\theta\right)^{1/4} \simeq \left(\frac{\lambda\sqrt{\rho R}}{\pi}\right)^{1/2} . \qquad (25)$$

The approximation on the right, which follows from Eq. (24), is very well satisfied for the glancing incidence modes of interest, and has been derived by other methods.[18,21] It is likely that for these small angles, the approximations made in the above approach by neglecting the difference in position and hence angle at which parts of the ray bundle at different heights strike the surface is comparable to the approximation made on the left in Eq. (25). This would certainly tend to smear out the position of the beam waist. For a true waveguide mode the beam would remain the same size everywhere, as predicted by the analysis in Refs. (18-21). On the other hand, for larger angles where the beam propagates by discrete bounces, one would expect the exact form of Eq. (25) to be more nearly valid, with the beam size oscillating between w_o halfway between bounces and a value w_1 at the wall, which by an extension of the above analysis is given by Eq. 25 with the term $(1 - \frac{R}{\rho}\sin^2\theta)^{1/4}$ in the denominator rather than in the numerator. For θ given by Eq. (14), the ratio of these two waist sizes differs from unity by $\sim(\lambda^2 R)^{1/3}/2\rho$, which is typically less than 10^{-2}.

The lens waveguide approach also predicts that a ray incident off-axis or with an initial slope will oscillate sinusoidally about the axis, with a displacement at the 2nth lens varying as $\cos n\psi$, where[46]

$$\psi = \cos^{-1}(2g^2 - 1) \quad , \tag{26}$$

provided that $0 < g^2 < 1$. The ray position therefore repeats whenever $\Delta n = 2\pi/\psi$, or after a distance

$$S = \Delta n\,(2L) = (2\pi/\psi)(4R \sin\theta) \quad . \tag{27}$$

Substituting g from Eq. 23 into Eq. 26 gives

$$\psi \cong 4\sqrt{\frac{R}{\rho}}\sin\theta \quad , \tag{28}$$

which together with Eq. 27 yields

$$S = 2\pi\sqrt{\rho R} \quad . \tag{29}$$

There is a nearly universal urge after deriving this pleasing result to cut open a curved section of copper tubing and photograph the sinusoidal trajectory of a He-Ne laser on the surface. Such a photo is shown in Fig. 5a, and similar photos appear in Refs. 18, 21. The measured oscillations period is in agreement with Eq. 29, within the uncertainty with which ρ and R can be determined after sawing open the tubing.

A parallel bundle of rays brought by a cylindrical lens to a line focus near the entrance to this guiding surface is shown in Fig. 5b. The periodic focusing of this beam is clearly seen, with only slight degradation after a few focuses, despite what might be considered a severely astigmatic geometry. The basic reason for this is that although, as noted earlier, rays entering at different heights strike the surface at different azimuthal

positions and hence with different values of θ, the number of bounces required to go through one period of oscillation increases as $1/\sin\theta$ while the chord length decreases as $\sin\theta$, resulting in Eq. 29 which is independent of θ. This result holds so long as θ is sufficiently small that the approximation leading to Eq. 28 is valid. Although this is obtained by basically a small angle expansion of $\cos\psi$, there is a near equality for terms up to ψ^4. Numerical evaluation indicates that Eq. 28 is in error by less than 5% for $\psi = \pi/2$.

It is interesting to note that while Lord Rayleigh ascribed the major part of the whispering gallery phenomenon in St. Paul's Cathedral to the cylindrical confinement treated in the previous section, he did mention that the dome could have some contribution to the effect.[15] We see from the above analysis that such an additional curvature can have an important effect on confining the wave in its transverse dimension.

One additional result is readily obtained by this lens waveguide approach. For the slightly curved parallel-plate structure of separation d, radius ρ studied in Refs. (12-14), the central ray trajectory is that of the mode of the parallel-plate structure which can be treated as composed of two plane wave which propagate at an angle $\sin\theta = k_x/k = \lambda/2d$ with respect to the walls. The distance measured along the ray between reflections is $L = d/\sin\theta$, and the effective focal length is again $f = \rho/2\sin\theta$, giving $g = 1 - d/\rho$ from Eq. 23. Substituting this value of g in Eq. 25 gives

$$w_o = \frac{2^{1/4}}{\sqrt{n}} (\rho d^3)^{1/4} (1 - d/2\rho)^{1/4}$$

$$\simeq \frac{2^{1/4}}{\sqrt{n}} (\rho d^3)^{1/4} \qquad (30)$$

This has the same functional form as the relation given in Ref. (13), but comparison with their numerical factor is not possible because of some uncertainity in their definition of beam width.

For small values of ρ, one expects additional propagation loss due to the fact that a plane-polarized beam will have a non-zero component perpendicular to the wall. Since the mode size increases only as $\rho^{\frac{1}{2}}$, this can be minimized by keeping to reasonably large values of ρ. Furthermore, for the circular guide the polarization tends to follow the surface curvature,[10] and it has been proposed that an input beam can be decomposed into polarization eigenstates, one of which will exhibit low loss propagation.[47] This is an area which merits further investigation.

IV. EXPERIMENTAL

A number of prototype structures have been investigated in order to test the theoretical predictions described above. A measurement of the guide loss was of particular importance since, while measurements on aluminum waveguides reported in Refs. 7-11 were in agreement with the form of Eq. 4, the actual losses measured were much higher than expected from the normal incidence reflectivity. To check this relation, entrance and exit slots were cut in a 23-cm diameter polished brass cylinder as shown in Fig. 6. A transmission of 53% was measured for a 10.6 μm CO_2 laser beam passed five times around the surface in a helical path. For this large a loss, it is necessary to exponentiate Eq. 4. The transmitted intensity after $\phi/2\theta$ reflections is

$$I = I_o (1 - A_N \sin \theta)^{\phi/2\theta} \quad , \tag{31}$$

or, for the small angles of interest for whispering mode propagation,

$$I = I_o e^{-A_N \phi/2} \tag{31a}$$

This latter expression gives, using the measured near-normal incidence reflectivity of 94.9%, a predicted throughput of 45%, which is lower than the 53% which was measured. Although some possibility for error exists in this reflectivity measurement, which was made by mode-matching the laser to the concentric cavity formed by the cylinder walls, and bouncing the beam within ~5% of normal incidence a number of times from one end of the cylinder to the other, it is believed that all or nearly all of the specularly reflected beam was collected on the Scientech power meter used for these measurements, and that this serendipitous departure from Eq. 31a has another explanation which will be discussed following a summary of some of the other experimental findings.

This cylinder was next plated with copper to give a measured reflectivity of 98.7% and a transmission of 79%, compared to a transmission of 82% given by Eq. 31a. The copper plating, in addition to increasing the intrinsic surface reflectivity, was done using a "brightener" which has the effect of leveling out small-scale surface roughness, and gave an improved surface finish as judged by the scattered light from a reflected He-Ne laser. Neither the original polished surface nor the plated surface could be considered as being of high optical quality, however. A similar structure is being prepared by diamond turning to produce a high quality optical finish, and results will be reported when available. This is of particular interest since diamond-turned surfaces have been measured as

having reflectivities higher than those given by the optical constants in Ref. 32,[48] with reflectance values of diamond-turned copper and silver of ~0.993 which approach the best values obtained by ultra-high-vacuum and ultra-clean sputtering techniques.[49-52] Even further improvement can be expected at low temperature.[53] Losses of ~2% or lower per revolution may be achievable with such fabrication methods.

Another prototype structure investigated was a 4½-turn section of commercial 5/16" ID copper tubing. Despite the fairly coarse surface texture and a radius ρ so short that the linearly polarized input beam had a significant component normal to the wall, a throughput of 40% was measured for this structure, and a reasonably clean mode of the type described above could be propagated. As a next attempt to achieve better surface quality, a 10-cm radius contour was rolled into a section of 0.467" square cross section magnet winding conductor. Unfortunately, in the initial attempt the deformation of the surface was not sufficient to eliminate the graininess and other surface defects of the starting material, and the finished surface scattered a He-Ne beam fairly strongly. The measured near-normal-incidence reflectivity was 92.4%, giving a predicted transmission for a single turn of 79%, compared to a measured transmission of 83%. Despite these initially disappointing results, the hope remains that with proper materials processing this technique will be capable of producing long lengths of low-loss waveguide.

The periodic repeat distance and mode size for this structure again appeared to be consistent with the theoretical considerations outlined above. This structure was also used to confirm the result described in Ref. 19 that the wave will follow the surface of the guide even if the surface is given a lateral deformation. A He-Ne beam appears "tied" to

the surface as the pitch of this single helical turn is altered. However, for this relatively gentle curvature, a twist of the surface will cause the beam to walk off the guide.

The results above and those reported in Ref. 34 for a brass guiding surface give a transmission in general agreement with, and in some instances higher than, that predicted by Eq. 31a. The measurements summarized in Ref. 11 give a loss for aluminum waveguides which is nearly six times larger than predicted from the normal incidence reflectivity. The authors ascribe this difference to scattering from surface irregularities. However, from the description of their surfaces, it would appear that they are of better optical quality than many of the copper surfaces described above. Moreover, one would expect the loss due to scattering to decrease near grazing incidence, the specular reflectivity being theoretically given by[54]

$$R = R_o \, e^{-(4\pi\sigma \sin\theta/\lambda)^2} \quad , \tag{32}$$

where σ is the rms surface roughness. It should be noted, however, that even the normal incidence ($\theta = 90°$) form of this relation does not appear to be well obeyed in the infrared.[48,56] Furthermore, at glancing incidence, the surface roughness may cause the wave to locally have a polarization component perpendicular to the surface, which is highly lossy. Nevertheless, these considerations may explain the result that some surfaces with large scattered light measured here gave higher transmission than predicted by Eq. 31a.

A more likely explanation for the large loss experienced with aluminum is the existence of a thin layer of Al_2O_3, even on non-anodized surfaces.

Although thin oxide layers are generally considered to have negligible effect on the TE reflectivity R_s, even for glancing incidence,[26] anomalous behavior is observed on the high frequency side of reststrahl frequencies,[57,58] where the real part of the index of refraction is less than one. This is the case for Al_2O_3 at 10.6 μm.[59] For angles of incidence beyond the critical angle for total reflection, the wave reaching the metal surface is evanescent, and it should not be surprising to find that the reflectivity is dependent on the film properties. It should be remembered that if the normal incidence loss is 2%, the loss at $\theta = 1°$ is only 3.5×10^{-4}, so that a loss six times as great would only be 0.2%. Increased TE losses larger than this have been calculated for larger values of θ, but for much thicker films.[57] The surface roughness may again play a role in producing some TM component of polarization, which can couple to surface plasmons under these conditions.[60]

Some very brief experiments were carried out with a not-very-specular piece of aluminum shimstock having a measured normal incidence reflectivity of ∿95%. With the material bent into a 180° loop, a 10.6 μm beam sent in so as to make the 180° turn in six bounces gave a measured throughput of 92%, in reasonable agreement with Eq. 31. As the beam was brought closer to grazing incidence, the transmission dropped to ∿60%. This type of behavior is not observed for copper. Some check on the role of surface roughness and of the oxide layer could be obtained by repeating this experiment with evaporated coatings with and without a non-reststrahl protective coating.[61]

Another set of experiments were performed to investigate coupling into a single radial mode. It is noted in Ref. 9 that the mode purity of the output of a waveguide can be maintained even if the waveguide is bent,

provided a gradual transition is made between the straight and bent sections. The argument is made on intuitive grounds that "gradual" means that the change in radius should not introduce a large change in mode width over a distance short compared to a diffraction length ($\sim\pi w^2/\lambda$). To test this, a piece of polished copper sheet was bent so as to go gradually from a straight section to a bent section and back to a straight section. The sheet was then cut in half at the minimum radius, which was ~12 cm, and a piece of brass shimstock was taped to each copper sheet to form the inner wall of a waveguide by means of two thicknesses of ~1-mm-thick spongy double-faced tape. The pieces of tape were sufficiently far apart that the CO_2 beam, which was mode-matched with a cylindrical lens into the waveguide, did not interact with them. It was found that the CO_2 beam exiting from the bent section of one waveguide was indeed confined very close to the outer wall and that it could be made to leave the waveguide in a fairly clean single lobe, as shown in Fig. 7a, particularly if the beam was focused slightly nearer to the outer wall. The necessity for this beam displacement may be caused by an insufficiently gradual bend. The second waveguide was then carefully positioned at the output of the first, so as to bring the beam back into a straight guide section. The burn pattern from the output mode shown in Fig. 7b looks nearly identical to the input beam at the same distance from the guide, except for some growth in the vertical direction.

One other result became apparent from these experiments: it was noted that virtually as good a mode could be propagated along the inner surface of the brass shimstock as inside the waveguide. This made it possible to measure the radial intensity distribution by moving an obstacle up to the

guide and measuring the change in energy transmitted as the obstacle was moved away from the surface in one-mil increments. The resulting intensity distribution is shown in Fig. 8, and closely approximates the form expected from Fig. 3 for the lowest-order mode. The value of a_b predicted by Eq. 13 is 0.126 mm. The measured half-width, which is comparable to this, is 5.8 mils, or 0.147 mm, in reasonable agreement. Thus we see that these radial mode properties follow theoretical expectations, and furthermore that it is possible to couple into a fairly clean single mode. If this is not done with sufficient care, however, the output shows a strong interference pattern between a number of modes.

V. CONCLUSIONS

The mode properties and guide losses discussed in sections II and III are in substantial agreement with experiment, and it appears that it should be possible to fabricate long low-loss whispering-mode waveguides. A more detailed investigation of the effects of surface properties on guide loss is in order.

ACKNOWLEDGMENTS

I would like to thank John Carlsten for a number of stimulating conversations, and Elsa Garmire for a helpful discussion and for bringing Ref. 18 to my attention. The continuing fabrication assistance of Dick Rhorer, Walt Zimmer, Warren Doty, and Bill Watson is appreciated.

REFERENCES

1. E. A. J. Marcatili and R. A. Schmeltzer, "Hollow metallic and dielectric waveguides for long distance optical transmission and lasers," Bell Syst. Tech. J. 43, 1783 (1964).

2. R. L. Abrams, "Waveguide gas lasers," in Laser Handbook, Vol. 3, ed. by M. L. Stitch, North Holland, 1979, p. 41, and references therein.

3. M. A. Guerra, A. Sanchez, and A. Javan, "$v = 2 \rightarrow 1$ absorption spectroscopy of vibrationally heated NO molecules using optical pumping in a waveguide," Phys. Rev. Lett. 38, 48[illegible] '77).

4. M. Yamanaka, "Optical[illegible] waveguide lasers," J. Opt. Soc. Am. 67, 952 (1977).

5. P. Rabinowitz, A. Kaldor, R. Brickman, and W. Schmidt, "Waveguide H_2 Raman laser," Appl. Opt. 15, 2005 (1976).

6. N. A. Kurnit, G. P. Arnold, L. M. Sherman, W. H. Watson, and R. G. Wenzel, "CO_2-pumped p-H_2 rotational Raman amplification in a hollow dielectric waveguide," Conference on Lasers and Electro-optic Systems, CLEOS/ICF '80, San Diego CA, Feb. 1980.

7. E. Garmire, T. McMahon, and M. Bass, "Propagation of infrared light in flexible hollow waveguides," Appl. Opt. 15, 145, 2028 (Erratum)(1976).

8. ____, "Flexible infrared-transmissive metal waveguides," Appl. Phys. Lett. 29, 254 (1976).

9. ____, "Low-loss optical transmission through bent hollow waveguides," Appl. Phys. Lett. 31, 92 (1977).

10. ____, "Low-loss propagation and polarization rotation in twisted infrared metal waveguides," Appl. Phys. Lett. 34, 35 (1979).

11. ____, "Flexible infrared waveguides for high-power transmission, IEEE J. Quant. Electron., QE-16, 23(1980).

12. T. Nakahara and N. Kurauchi, "Guided beam waves between parallel concave reflectors," IEEE Trans. on Microwave Theory and Techniques, MTT-15, 66 (1967).

13. H. Nishihara, T. Inoue, and J. Koyama, "Low-loss parallel-plate waveguide at 10.6 μm," Appl. Phys. Lett. 25, 391 (1974).

14. H. Nishihara, T. Mukai, T. Inoue, and J. Koyama, "Self-focusing parallel-plate waveguide CO_2 laser with uniform transverse excitation," Appl. Phys. Lett. 29, 577 (1976).

15. Lord Rayleigh (J. W. Strutt), Theory of Sound, §287, MacMillan, 1894, Vol. 2, p. 126.

16. ____, "The problem of the whispering gallery," Phil. Mag. 20, 1001 (1910) (Scientific Papers, Vol. 5, Cambridge Univ. Press, 1912, p. 617).

17. ____, "Further application of Bessel's functions of high order to the whispering gallery and allied problems," Phil. Mag. 27, 100 (1914) (Scientific Papers, Vol. 6, Cambridge Univ. Press, 1920, p. 211).

18. M. E. Marhic, L. I. Kwan, and M. Epstein, "Optical surface waves along a toroidal metallic guide," Appl. Phys. Lett. 33, 609 (1978).

19. ____, "Invariant properties of helical-circular metallic waveguides," Appl. Phys. Lett. 33, 874 (1978).

20. ____, "Whispering-gallery CO_2 laser," IEEE J. Quantum Electron. QE-15, 487 (1979).

21. L. W. Casperson and T. S. Garfield, "Guided beams in concave metallic waveguides," IEEE J. Quantum Electron. QE-15, 491 (1979).

22. E. A. J. Marcatili, "Bends in optical dielectric guides," Bell Syst. Tech. J. 48, 2103 (1969).

23. S. Sheem and J. R. Whinnery, "Guiding by single curved boundaries in integrated optics," Wave Electronics 1, 61 (1974/75).

24. ____, "Modes of a curved surface waveguide for integrated optics," Wave Electronics 1, 105 (1974/75).

25. J. Bremer and L. Kaihola, "An x-ray resonator based on successive reflections of a surface wave," Appl. Phys. Lett. 37, 361, 1051 (Erratum) (1980).

26. R. G. Greenler, "Infrared study of adsorbed molecules on metal surfaces by reflection techniques," J. Chem. Phys. 44, 310 (1966).

27. R. W. Hannah, "An optical accessory for obtaining the infrared spectra of very thin films," Appl. Spectroscopy 17, 23 (1963).

28. G. W. Poling, "Infrared reflection studies of the oxidation of copper and iron," J. Electrochem. Soc. 116, 958 (1969).

29. E. Garmire, "Propagation of IR light in flexible hollow waveguides: Further discussion," Appl. Opt. 15, 3037 (1976).

30. K. D. Laakmann and W. H. Steier, "Waveguides: characteristic modes of hollow rectangular dielectric waveguides," Appl. Opt. 15, 1334, 2029 (Erratum)(1976).

31. M. Born and E. Wolf, Principles of Optics, 3rd ed., Pergamon, 1965, p. 617. Because we are concerned with grazing incidence, θ is measured from the surface tangent rather than the normal as in this reference.

32. G. Hass and L. Hadley, "Optical properties of metals," American Institute of Physics Handbook, 3rd Ed., McGraw-Hill, 1972, Sec. 6g, p. 6-134.

33. H. Krammer, "Propagation of modes in curved hollow metallic waveguides for the infrared," Appl. Opt. 16, 2163 (1977).

34. ____, "Light waves guided by a single curved metallic surface," Appl. Opt. 17, 316 (1978).

35. J. B. Keller and S. I. Rubinow, "Asymptotic solutions of eigenvalue problems," Annals of Phys. 9, 24 (1960).

36. M. Heiblum and J. H. Harris, "Analysis of curved optical waveguides by conformal transformation," IEEE J. Quantum Electron., QE-11, 75 (1975).

37. M Abramowitz and I. A. Stegun, Handbook of Mathematical Tables, NBS Applied Mathematics Series #55, 1964, p. 446.

38. K. G. Budden, The Wave-Guide Mode Theory of Wave Propagation, Logos, London, 1961, Ch. 11.

39. J. R. Waite, "Light waves guided by a single curved surface: comment," Appl. Opt. 17, 1678 (1978).

40. Ref. 38, pp. 180, 183.

41. Ref. 38, p. 181.

42. J. R. Pierce, "Modes in sequences of lenses," Proc. Nat'l. Academy of Sciences, 47, 1808 (1961).

43. A. E. Seigman, An Introduction to Lasers and Masers, McGraw-Hill, 1971, Ch. 8 and references therein.

44. F. A. Jenkins and H. A. White, Fundamentals of Optics, 3rd Ed. McGraw-Hill, 1957, p. 95.

45. Ref. 43, p. 323.

46. Ref. 43, p. 299.

47. M. E. Marhic, "Polarization and losses of whispering-gallery waves along twisted trajectories," J. Opt. Soc. Am. 69, 1218 (1979).

48. D. L. Decker, J. M. Bennett, M. J. Soileau, J. O. Porteus, and H. E. Bennett, "Surface and optical studies of diamond-turned and other metal mirrors," Optical Eng. 17, 160 (1978).

49. J. M. Bennett and E. J. Ashley, "Infrared reflectance and emittance of silver and gold evaporated in ultrahigh vacuum," Appl. Opt. 4, 221 (1965).

50. H. E. Bennett and J. M. Bennett, "Validity of the Drude theory for silver, gold, and aluminum in the infrared," in Optical Properties and Electronic Structure of Metals and Alloys edited by F. Abeles, North-Holland, 1966, pp. 175-188.

51. H. E. Bennett, J. M. Bennett, E. J. Ashley, and R. J. Motkya, "Verification of the anomalous-skin-effect theory for silver in the infrared," Phys. Rev. 165, 755 (1968).

52. P. A. Temple, D. K. Burge, and J. M. Bennett, "Optical properties of mirrors prepared by ultraclean dc sputter deposition," in Laser-Induced Damage in Optical Materials, 1976, A. J. Glass and A. H. Guenther, eds. (NBS Special Publication 462) pp. 195-201.

53. W. M. Toscano and E. G. Cravalho, "Thermal radiative properties of the noble metals at cryogenic temperatures," Journal of Heat Transfer, Trans. ASME Series C 98, 438 (1976) and references therein.

54. Ref. 51, Eq. 21 with θ replaced by 90-θ.

55. H. E. Bennett and J. O. Porteus, "Relation between surface roughness and specular reflectance at normal incidence," J. Opt. Soc. Am. 51, 123 (1961).

56. H. E. Bennett, "Scattering characteristics of optical materials," Opt. Eng. 17, 480 (1978).

57. J. T. Cox, G. Hass, and W. R. Hunter, "Infrared reflectance of silicon oxide and magnesium fluoride protected aluminum mirrors at various angles of incidence from 8 μm to 12 μm," Appl. Opt. 14, 1247 (1975).

58. J. T. Cox and G. Hass, "Aluminum mirrors Al_2O_3-protected, with high reflectance at normal, but greatly decreased reflectance at higher angles of incidence in the 8-12-μm region," Appl. Opt. 17, 333 (1978).

59. H. G. Häfele, "Das Infrarotspektrum des Rubins," Z. Naturforsch. A, 18, 331 (1963).

60. A. Otto, "Excitation of nonradiative surface plasma waves in silver by the method of frustrated total reflection," Z. Physik 216, 398 (1968).

61. J. T. Cox and G. Hass, "Protected Al mirrors with high reflectance in the 8-12 μm region from normal to high angles of incidence," Appl. Opt. 17, 2125 (1978).

FIGURE CAPTIONS

Figure 1. Scheratic of helical configuration of doubly-curved whispering-mode waveguide.

Figure 2. Ray trajectories with cylindrical boundary.

Figure 3. Radial mode profile. For mth mode, wall is at mth zero, ξ_m, of Ai(x).

Figure 4 Focusing properties of doubly-curved structure and equivalent lens waveguide.

Figure 5. (a). Photograph of sinusoidal trajectory of He-Ne laser propagating along cut-open section of copper tubing having $\rho \sim 0.87$ cm, $R \sim 32$ cm. Camera was located near center of curvature of tube. (b). Similar photograph with parallel vertical ray bundle incident on surface, showing periodic focusing of beam. Beam width is ~ 7 mm in vertical direction. Edges of copper tubing are more evident in this photo.

Figure 6. Structure used for measurement of transmission through a number of helical turns around a cylindrical surface.

Figure 7. Burn patterns of mode taken ~ 15 cm from waveguide output. (a) Output from bent section. (b) Output from second waveguide which brings mode back into straight section. Whitened center is response of burn paper to higher intensity.

Figure 8. Radial mode distribution measured on beam propagated along wall which is gradually bent from $R = \infty$ to $R = 12$ cm.

DOUBLY-CURVED "RIBBON" WHISPERING-MODE WAVEGUIDE

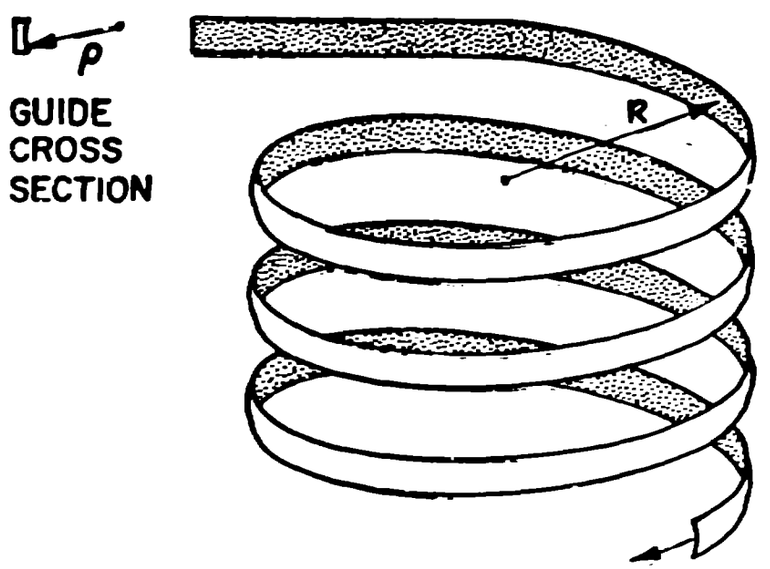

APPLICATIONS

RAMAN OSCILLATOR
OPTICALLY PUMPED LASER
LONG-PATH ABSORPTION CELL

ADVANTAGES

SMALL MODE VOLUME ⇒
LOW PUMP ENERGY
LONG LENGTHS IN A SMALL
VOLUME
LOSS / REVOLUTION ≃ π × NORMAL-
INCIDENCE LOSS

LOnly this part will be used in Fig 1 in paper. The rest will be used in poster presentation.

Fig. 1

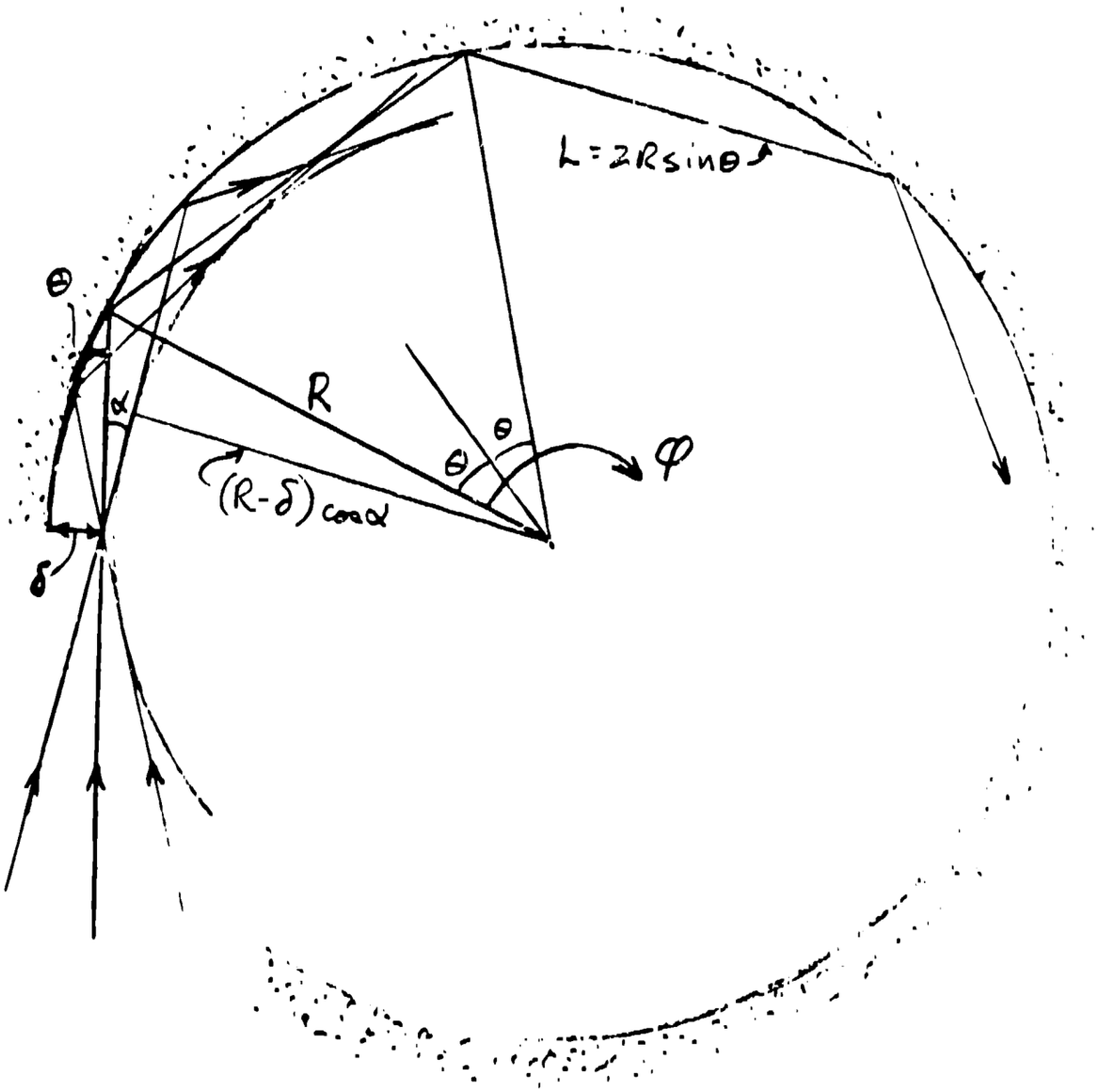

Fig. 2

RADIAL MODE PROFILE

$$E_m \sim Ai\left[\left(\frac{2k^2}{R}\right)^{1/3}(R-r) + \xi_m\right]$$

$$\text{Width} \sim \left(\frac{R}{2k^2}\right)^{1/3}\xi_m \approx \frac{1}{2}(\lambda^2 R)^{1/3}\left[\frac{3}{2}(m-1/4)\right]^{2/3}$$

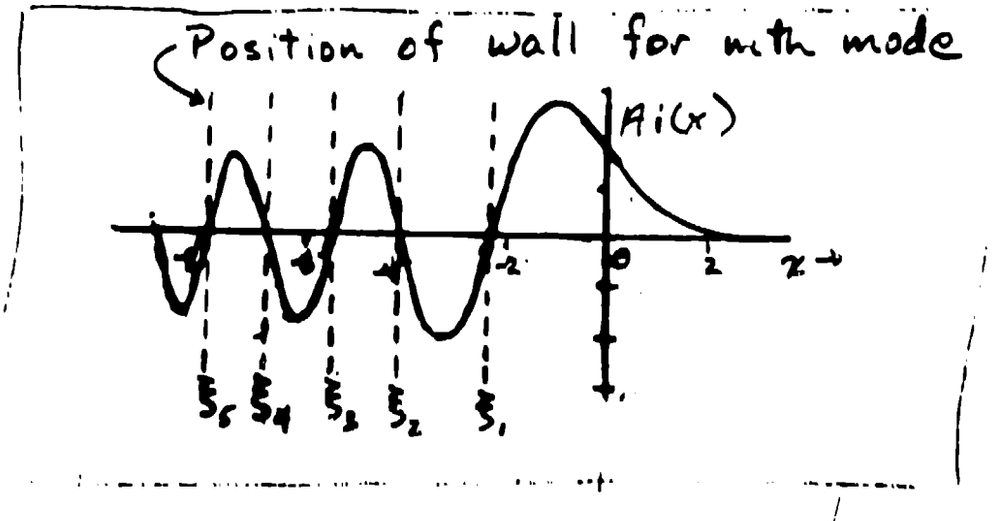

Fig. 3

Only this part will be used in Fig 3, the rest will be used in later processing.

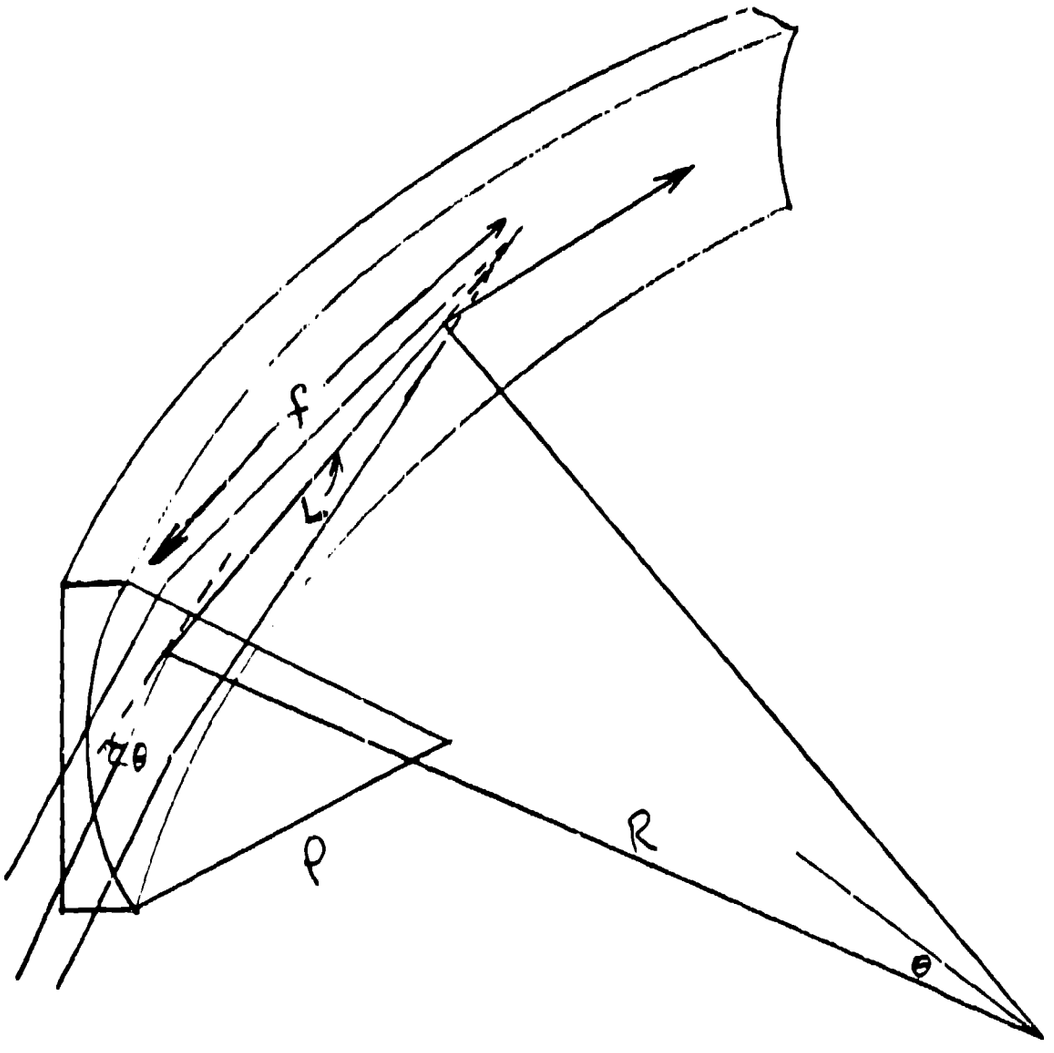

EQUIVALENT LENS WAVEGUIDE:

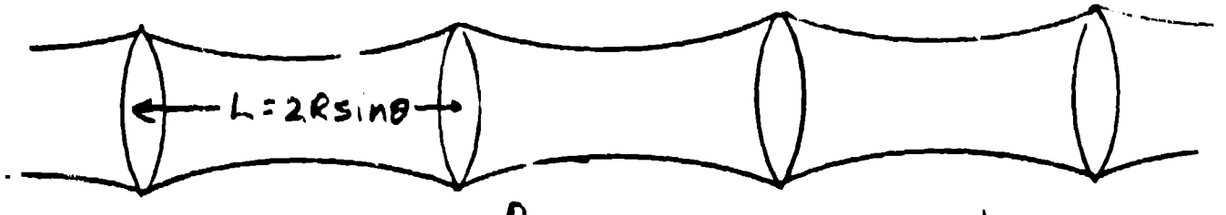

$$f = \frac{\rho}{2\sin\theta} \qquad g = 1 - \frac{L}{2f}$$

$$W_0 = \left(\frac{L\lambda}{2\pi}\right)^{1/2}\left(\frac{1+g}{1-g}\right)^{1/4} = \left(\frac{\lambda\sqrt{\rho R}}{\pi}\right)^{1/2}\left(1 - \frac{R}{\rho}\sin^2\theta\right)^{1/4} \approx \left(\frac{\lambda\sqrt{\rho R}}{\pi}\right)^{1/2}$$

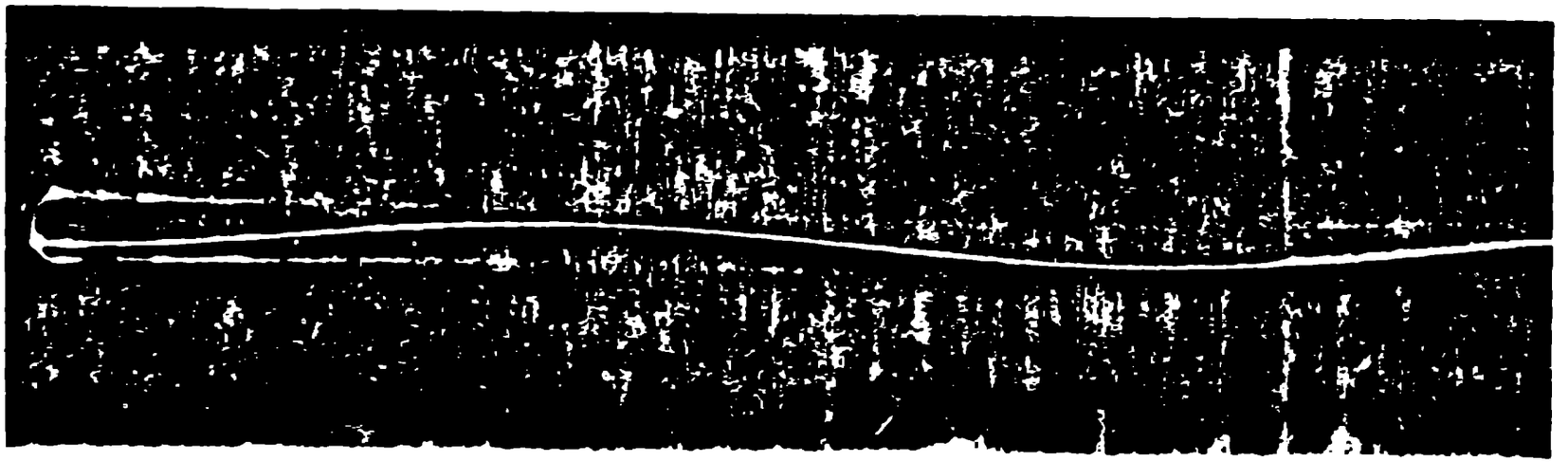

(a)

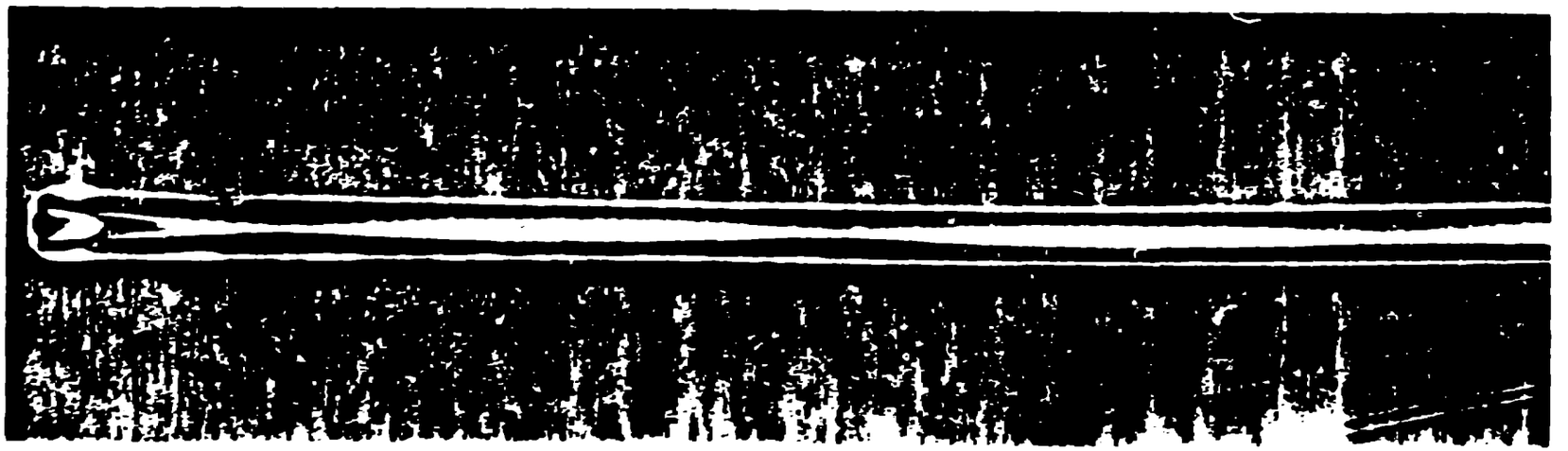

(b)

FIG. 5

WHISPERING-MODE WAVEGUIDE

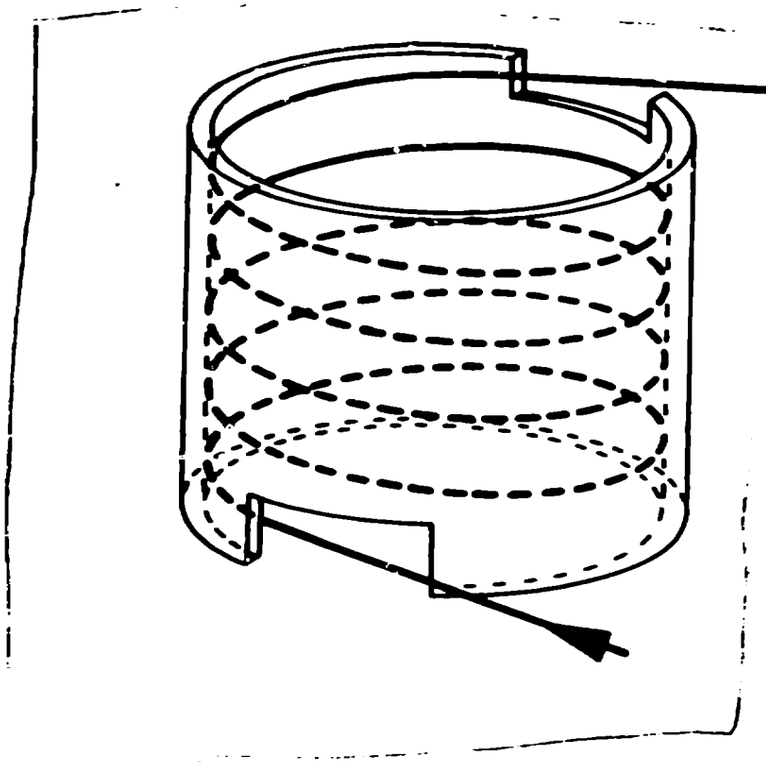

HAVE MEASURED ~~53%~~ 79%
THROUGHPUT OF 10.6 μm
FOR 5 TURNS AROUND
~~POLISHED BRASS~~ COPPER PLATED
CYLINDER WITH
R_1 = ~~95%~~ 98.7%

Only this part will be used in Fig. 6 in paper, the rest will be used in [illegible]

Fig 6

AP-1-VG-6396

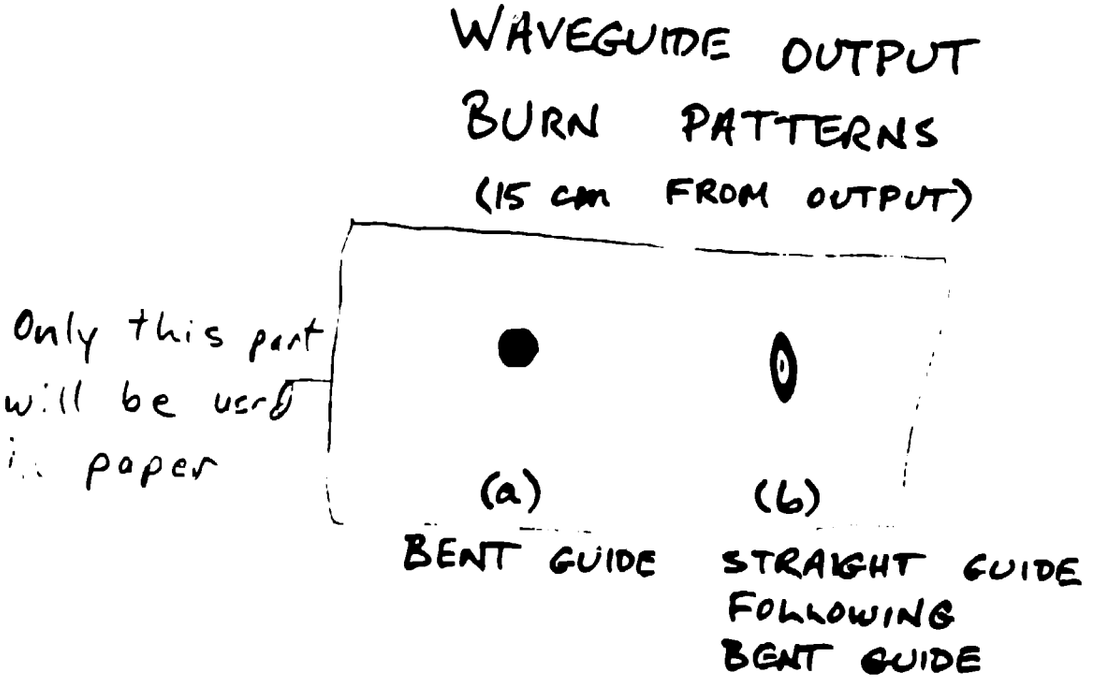
WAVEGUIDE OUTPUT
BURN PATTERNS
(15 cm FROM OUTPUT)
Only this part will be used in paper
(a)
BENT GUIDE
(b)
STRAIGHT GUIDE FOLLOWING BENT GUIDE

FIG. 7

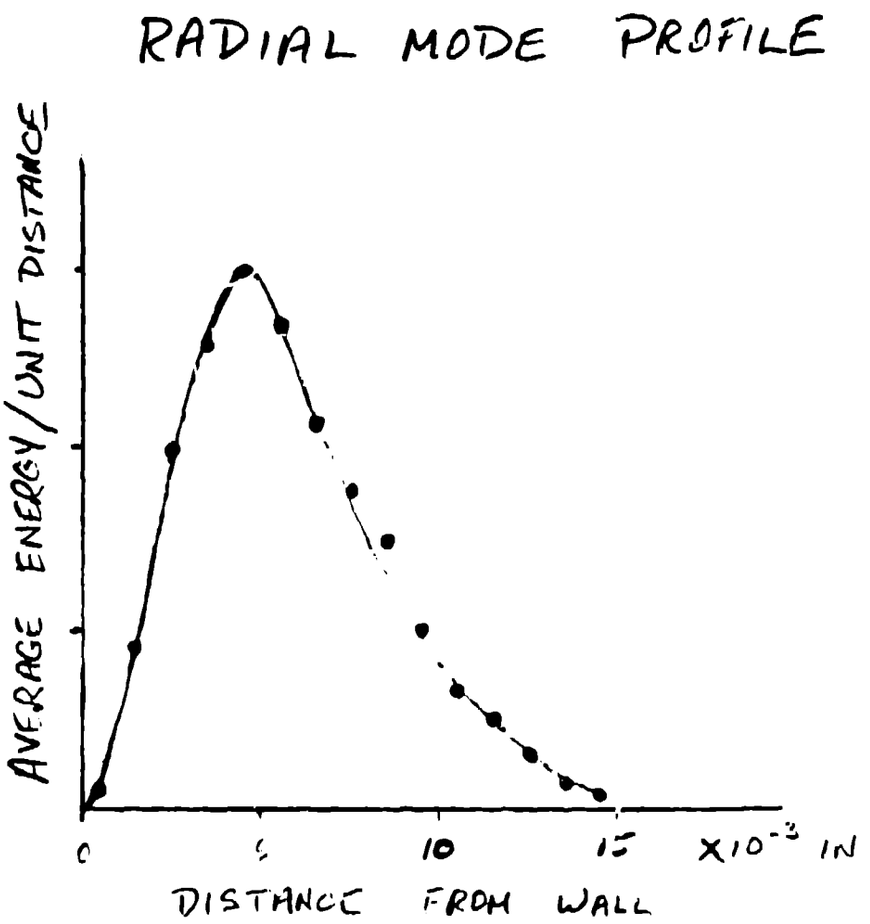
RADIAL MODE PROFILE
AVERAGE ENERGY/UNIT DISTANCE
0
5
10
15
X10⁻³ IN
DISTANCE FROM WALL

FIG. 8

WAVEGUIDE LOSS:

$$r_s = \frac{\sqrt{v^2 - \cos^2\theta} - \sin\theta}{\sqrt{v^2 - \cos^2\theta} + \sin\theta} \approx \frac{v - \sin\theta}{v + \sin\theta}$$

$(v = \eta - iK,\ |\eta^2 - K^2| >> 1)$

$$A^{TE}(\theta) = 1 - |r_s|^2 \cong \frac{4\,\mathrm{Re}(v)\sin\theta}{|v + \sin\theta|^2}$$

$$\cong A_N \sin\theta$$

FOR A BEND OF ANGLE Φ,

$$A_B(\theta) = \frac{\Phi}{2\theta} A^{TE}(\theta) = \frac{\Phi}{2\theta} A_N \sin\theta$$

$$\approx \frac{A_N \Phi}{2}$$

(For poster presentation only)